

independent of X. Consequently, the relative differences between the ΔH_f values should be meaningful and clearly indicate that the dihalogen adducts should be thermodynamically more stable than the dihydrogen adduct.¹⁷

Structural data for Pt_2X , as well as for Pt_2X_2 species, indicate that both the Pt-Pt and the Pt-X bond lengths increase in the order $Cl < Br < I$.¹⁸ Resonance Raman spectral measurements on Pt_2X ($\sigma^2\sigma^*1$) and Pt_2X_2 (σ^2) indicate a decrease in the Pt-Pt and Pt-X vibrational frequencies in the order $Cl > Br > I$,¹⁸ a trend ascribed to differences in electron donation from the axial ligand X⁻ in Pt_2X (or Pt_2X_2) into the Pt-Pt $d\sigma^*$ orbital. These results suggest that $D_0(Pt_2X)$ should decrease in the order $Cl > Br > I$. The experimental PAC results indicate a similar ordering for $D_0(Pt_2X)$, $Cl > Br \sim I$. The similar calculated bond dissociation energies of Pt_2Br and Pt_2I are somewhat unexpected but perhaps can be explained by competing excited-state processes of Pt_2^* .¹⁰

The Pt_2^* excited triplet state is one of the most reactive metal-centered radicals toward atom-transfer reactions.¹ The reactions of Pt_2^* are highly exothermic (ΔH_2 , Table I), in part because of the extremely strong Pt-X bonds that are formed by Pt_2^* , as indicated earlier. Although factors other than reaction exothermicity are important in determining the absolute rates of atom abstraction, several observations can perhaps be made.

First, Pt_2^* , with its $d\sigma^*$ electron, is electronically similar to alkyl, hydroxyl, or other metal-centered radicals such as $Mn(CO)_5$. However, the reactivities of these species toward atom abstraction can be quite different. These differences can potentially be related to reaction enthalpy or bond strength differences. For example, whereas the rates of hydrogen atom abstraction by Pt_2^* , *t*-BuO[•] radical, and also $n\pi^*$ excited states of ketones are similar, those of other metal-centered radicals are somewhat slower.^{1b,19} As indicated earlier, these metal-hydrogen bonds are considerably weaker than the Pt-H and RO-H hydrogen bonds, ~ 103 kcal/mol.^{11,14,20} The significantly faster rate of Cl abstraction from CCl_4 by Pt_2^* , 2×10^9 M⁻¹ s⁻¹,^{2b} than by CH_3^* , $\sim 10^3$ M⁻¹ s⁻¹,²¹ is possibly related to the difference between the Pt-Cl and the C-Cl bond strengths, 106 and 84.6 kcal/mol, respectively.

Second, halogen atom abstraction is apparently faster than hydrogen atom abstraction for a given reaction exothermicity. For example, iodine abstraction from C_6H_5I occurs significantly faster than hydrogen abstraction from $C_6H_5CH_2OH$, although both have similar ΔH_2 values. The faster rates for halogen abstraction may possibly indicate some charge-transfer character in the transition state.

Third, the rate constants for quenching of Pt_2^* by aryl halides (ArX) in methanol are in the order $I > Br > Cl$.^{2b} Although this trend may follow ArX bond strengths as previously suggested, it apparently does not simply follow the reaction exothermicities. The ΔH_2 values for the reaction of Pt_2^* with chloro-, bromo-, and iodobenzene are -10.6, -9.0, and -25.1 kcal/mol, on the basis of the appropriate $D_0(Pt_2X)$ values and the $D_0(RX)$ values of the aryl halides, 95.5 (Cl), 80.6 (Br), and 65.4 (I) kcal/mol.¹¹

Acknowledgment. This research was generously supported by grants from the National Science Foundation (CHE-9057092 and CHEM-9007673).

- (17) Alternatively, the instability of Pt_2H_2 relative to Pt_2X_2 may rather be kinetic in nature. In fact, the hydrogen and halogen adducts may decompose by quite different mechanistic pathways.
- (18) (a) Che, C.-M.; Herbstein, F. H.; Schaefer, W. P.; Marsh, R. F.; Gray, H. B. *J. Am. Chem. Soc.* **1983**, *105*, 4604. (b) Stein, P.; Dickson, M. K.; Roundhill, D. M. *J. Am. Chem. Soc.* **1983**, *105*, 3489. (c) Kurmoo, M.; Clark, R. H. *J. Inorg. Chem.* **1985**, *24*, 4420.
- (19) Gasanov, R. G.; Dotdaev, S. Kh. *Izv. Akad. Nauk SSSR, Ser. Khim.* **1986**, *9*, 1981.
- (20) Conner, J. A.; Zafarani-Moattar, M. T.; Bickerton, J.; El Saied, N. I.; Suradi, S.; Carson, R.; Al Takhin, G.; Skinner, H. A. *Organometallics* **1982**, *1*, 1166.
- (21) Edwards, F. G.; Mayo, F. R. *J. Am. Chem. Soc.* **1950**, *72*, 1265.
- (22) (a) Asano, T.; le Noble, W. J. *Chem. Rev.* **1978**, *78*, 407. (b) Van Eldik, R.; Asano, T.; le Noble, W. J. *Chem. Rev.* **1989**, *89*, 549.
- (23) Scaiano, J. C.; Stewart, L. C. *J. Am. Chem. Soc.* **1983**, *105*, 3609.

Contribution from the Departments of Chemistry,
The State University of New York at Buffalo,
Acheson Hall, Buffalo, New York 14214,
and The University of Mississippi, University, Mississippi 38677

Electrochemical Reduction of Dioxygen in Room-Temperature Imidazolium Chloride-Aluminum Chloride Molten Salts

Michael T. Carter,[†] Charles L. Hussey,[‡]
Sandra K. D. Strubinger,[‡] and Robert A. Osteryoung^{*,†}

Received August 6, 1990

Introduction

We report here the voltammetric behavior of dioxygen in a basic, room-temperature chloroaluminate molten salt, 1-ethyl-3-methylimidazolium chloride (ImCl) mixed with $AlCl_3$. Melts composed of mixtures of ImCl and $AlCl_3$ are basic, neutral, or acidic, depending on whether the mole ratio, $AlCl_3:ImCl$, is less than, equal to, or greater than 1, respectively. These melts and the closely related 1-*n*-butylpyridinium chloride- $AlCl_3$ systems have found wide application in studies of the electrochemistry of organic and inorganic species.¹⁻³ The electrochemistry of O_2 reduction has been the subject of numerous studies in aqueous, nonaqueous, and high-temperature molten salt systems. These have been reviewed in detail by Hoare.⁴ To our knowledge, this is the first report of the electrochemistry of O_2 in room-temperature melts.

Experimental Section

ImCl was prepared by a modification of a previously reported procedure.⁵ $AlCl_3$ (Fluka) was purified by sublimation. Anhydrous $FeCl_2$ (Alfa Products) was used as received. Melts were prepared by mixing appropriate quantities of ImCl and $AlCl_3$. All manipulations (e.g., preparation of melts, assembling of electrochemical cells) were performed inside a Vacuum Atmospheres Co. drybox, under an atmosphere of purified He.

All electrochemical experiments were performed outside of the drybox, in a gastight, single-compartment cell. The volume of melt used for electrochemical measurements was typically 20 mL. O_2 and Ar were passed through a drying column composed of molecular sieves and Drierite, before entering the cell. Gases were introduced into the melt via a gas dispersion tube immersed in the melt and were continuously passed over the melt during measurements.

The working electrodes were glassy carbon (geometric area = 0.071 cm²) and Pt (geometric area = 0.025 cm²) disks, obtained from Bioanalytical Systems. The electrodes were polished with 0.25- μ m diamond paste (Buehler, Ltd.) on a Nylon buffing pad and were cleaned ultrasonically in 95% ethanol prior to use. The counter electrode was a Pt wire. All potentials were measured with respect to an Al wire immersed in 1.5:1 (mole ratio of $AlCl_3:ImCl$) melt, denoted Al/Al(III). The reference electrode was separated from the working solution by a Vycor frit. All measurements were conducted at the ambient temperature of the laboratory (25 \pm 1 °C).

A Princeton Applied Research Model 273 potentiostat controlled by a Digital Equipment Corp. Model PDP-8/e computer was used in all experiments.

Results and Discussion

A typical cyclic staircase voltammogram (CSV), at a glassy-carbon disk electrode, of an O_2 -saturated 0.95:1 melt is shown in Figure 1A. Saturation of the melt, as indicated by the constancy of the cathodic peak height (i_{pc}) of the reduction wave with time, required ca. 30 min of vigorous bubbling with dry O_2 . O_2 is reduced in a single voltammetric wave with cathodic peak potential $E_{pc} = -0.7$ V vs Al/Al(III). No other redox processes are observed within the electrochemical window of the 0.95:1 melt (+1.0 to -1.8 V). The reduction wave could be eliminated by purging with dry Ar (Figure 1B). No reverse current was observed, following reduction, for sweep rates, v , $5 \leq v \leq 200$ mV/s. The peak current was a linear function of $v^{1/2}$ but with a positive

* To whom correspondence should be addressed.

[†] The State University of New York at Buffalo.

[‡] The University of Mississippi.

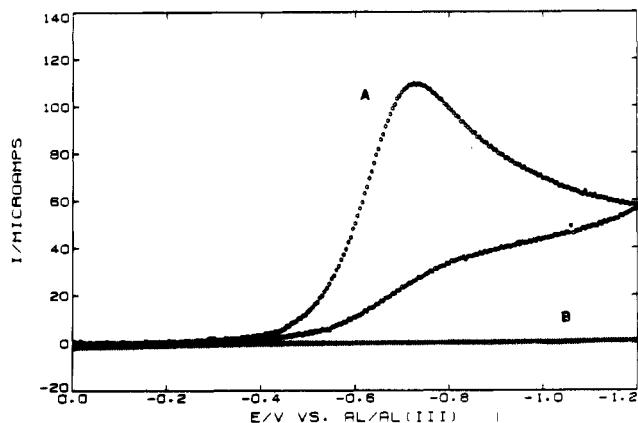


Figure 1. Cyclic staircase voltammogram of (A) O_2 -saturated and (B) Ar-saturated 0.95:1 melt. Conditions: working electrode, glassy carbon (geometric area = 0.071 cm^2); staircase step height = 5 mV; staircase frequency = 20 Hz; temperature = 24°C .

intercept on the current axis. This is probably a consequence of adsorption of O_2 onto the GC on the voltammetric time scale. On increasing v , the wave broadened (e.g., $|E_{pc} - E_{pc/2}| = 139 \text{ mV}$ at $v = 5 \text{ mV/s}$ and 175 mV at $v = 200 \text{ mV/s}$). E_{pc} shifted linearly by -50 mV/decade increase in v . Addition of a proton source (H_2O), caused a positive shift in E_{pc} . These results are consistent with a quasireversible electron transfer, followed by a fast, irreversible chemical reaction involving protons.⁶ The heterogeneous electron-transfer kinetics of O_2 reduction in the melt appear slow compared to those observed previously in nonaqueous systems. No electrochemical processes involving O_2 were observed in an acidic (1.5:1) melt.

The glassy-carbon electrode was slowly passivated with respect to O_2 reduction, following continuous voltammetric cycling, possibly by formation of aluminum oxide or oxychloride species, by reaction of $AlCl_4^-$ with the reduction product (e.g. H_2O_2 or H_2O). For example, following the initial CSV scan shown in Figure 1, successive cycles showed that the wave became broader and shifted to more negative potentials. The magnitude of i_{pc} also decreased. Additionally, the background processes (Im^+ reduction and Cl^- oxidation) were shifted to more extreme potentials. Continuous cycling through potentials positive enough to cause Cl_2 evolution did not improve the behavior of the electrode. If the glassy-carbon disk was allowed to remain in contact with the O_2 -saturated melt, but at open circuit, similar passivation was observed, within ca. 2 h of contact time. This required a much longer time than that for passivation during cycling. In an O_2 -saturated 1.5:1 melt, the electrode surface was affected in the same way but much more rapidly. Thus, it appears that the working electrode surface can be passivated both by formation of insulating products at the electrode surface, during cycling, and by slow oxidation of the electrode surface at open circuit. Similar results were also obtained at Pt electrodes. A visible film formed during cycling of the glassy-carbon electrode in the O_2 -saturated melts. The surface of the electrode could be wetted by water much more effectively than a freshly polished, hydrophobic surface. The original behavior of these systems could only be obtained after polishing the electrode and returning it to the melt.

A typical normal pulse voltammogram (NPV) of an O_2 -saturated 0.95:1 melt is shown in Figure 2. The NPV showed a pronounced maximum prior to the limiting current plateau (i_{lim}), indicative of adsorption of O_2 on the electrode surface.^{7a,b} The

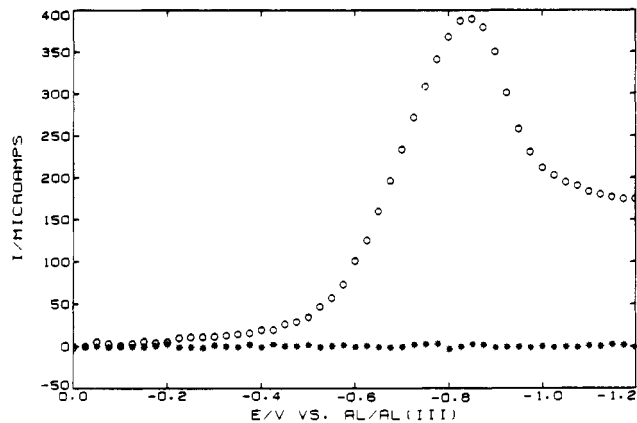
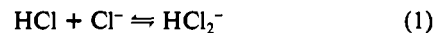


Figure 2. Normal pulse voltammogram of O_2 -saturated 0.95:1 melt. Conditions: pulse time = 20 ms; pulse step height = 25 mV. Other conditions are as in Figure 1. Circles represent currents at end of each pulse, and asterisks, the current prior to each pulse.

value of i_{lim} and that of the maximum were essentially independent of pulse time (t_p) for $t_p \leq 100 \text{ ms}$ (for step width = 25 mV) and linear with $t_p^{-1/2}$ for $t_p > 100 \text{ ms}$. In the latter case, plots of i_{lim} vs $t_p^{-1/2}$ had a significantly positive current axis intercept, consistent with the presence of adsorbed O_2 on the electrode surface.^{7a} At large t_p (e.g., 1 s) the current maximum was suppressed, but Nernst plots of the rising portion of the NPV curve were highly nonlinear. O_2 adsorption onto carbon has been documented previously.⁸ Adsorption of reactant at an electrode surface causes a large current maximum that is pulse time dependent. As t_p increases, the maximum is suppressed because of the difference in time dependence of current due to adsorption (t^{-1}) and diffusion ($t^{-1/2}$). The limiting current is depressed relative to that in the absence of adsorption due to depletion of reactant at the electrode surface.^{7b} Adsorption of O_2 here must be rather weak, since strong adsorption of the reactant would give rise to a postwave at potentials negative of the main reduction (in cyclic staircase voltammetry experiments), whereas weak adsorption would not.^{7c}

The concentration of O_2 was determined by mixing a weighed amount of O_2 -saturated melt with an excess of $FeCl_2$. A poised system with open circuit potential = $+0.233 \text{ V}$ was obtained, indicating an equilibrium mixture of Fe(II) and Fe(III) chloro complexes. E° of the Fe(II)/Fe(III) redox couple in this medium is $+0.267 \text{ V vs Al/Al(III)}$.⁹ No oxidation of Fe(II) was observed in a blank experiment in which Ar-saturated melt was used. In a basic melt, Fe(II) exists as $FeCl_4^{2-}$,^{9,10} which can act as a $1 e^-$ reductant. A composite NPV curve was constructed from two experiments involving pulses to more positive (Fe(II) oxidation) or more negative (Fe(III) reduction) potentials, initiated from the open circuit potential of the system. From the fraction of the total NPV current due to reduction of $FeCl_4^-$, the concentration of O_2 was estimated as 2.53 mM (based on $1 e^-$ reduction of O_2). Basic melts typically contain protonic impurities which exist in the equilibrium¹¹



In our case, approximately 8.5 mM proton was present. Thus, the saturation concentration of O_2 is probably closer to 0.63 mM , since the stoichiometry of the Fe(II): O_2 reaction, in the presence of a proton source, is at most 4:1. The maximum O_2 concentration determined here is comparable to that found in several organic solvents.¹²

- (1) Chum, H. L.; Osteryoung, R. A. In *Ionic Liquids*; Inman, D., Lovering, D. G., Eds.; Plenum: New York, 1981, pp 407-423.
- (2) Hussey, C. L. *Pure Appl. Chem.* **1988**, *60*, 1763.
- (3) Hussey, C. L. In *Advances in Molten Salt Chemistry*; Mamantov, G., Ed.; Elsevier: Amsterdam, 1983; Vol. 5, pp 185-230.
- (4) Hoare, J. P. In *Encyclopedia of Electrochemistry of The Elements*; Bard, A. J., Ed.; Marcel Dekker: New York, 1974; Vol. 2, pp 191-382.
- (5) Wilkes, J. S.; Levisky, J. A.; Wilson, R. A.; Hussey, C. L. *Inorg. Chem.* **1982**, *21*, 1263.
- (6) Nicholson, R. S.; Shain, I. *Anal. Chem.* **1964**, *36*, 706.

- (7) (a) Van Leeuwen, H. P. *J. Electroanal. Chem. Interfacial Electrochem.* **1982**, *133*, 201. (b) Flanagan, J. B.; Takahashi, K.; Anson, F. C. *J. Electroanal. Chem. Interfacial Electrochem.* **1977**, *85*, 257. (c) Wopschall, R. H.; Shain, I. *Anal. Chem.* **1967**, *39*, 1514.
- (8) Morcos, I.; Yeager, E. *Electrochim. Acta* **1970**, *15*, 953.
- (9) Nanjundiah, C.; Shimizu, K.; Osteryoung, R. A. *J. Electrochem. Soc.* **1982**, *129*, 2474. E° of Al/Al(III) in 1.5: $AlCl_3$: $ImCl$ = $+180 \text{ mV}$ vs 2:1 $AlCl_3$: $1-n$ -butylpyridinium chloride.
- (10) Laher, T. M.; Hussey, C. L. *Inorg. Chem.* **1982**, *21*, 4079.
- (11) Zawodzinski, T. A.; Osteryoung, R. A. *Inorg. Chem.* **1988**, *27*, 4383.

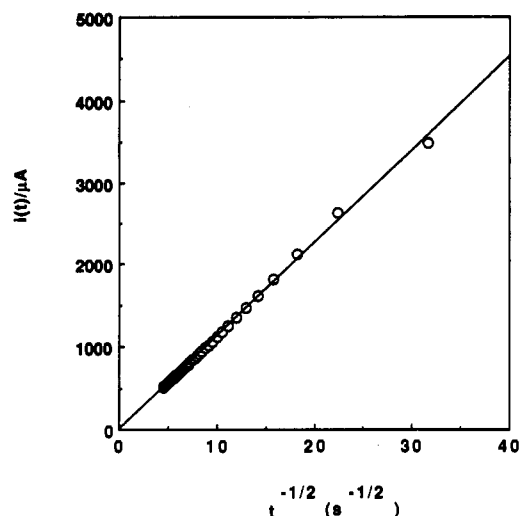
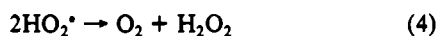
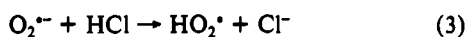


Figure 3. Chronoamperometry of O_2 -saturated 0.95:1 melt. Potential step was from 0.0 to -1.2 V vs Al/Al(III) for 50 ms. Other conditions are as in Figure 1.

The fact that O_2 is capable of oxidizing $FeCl_4^{2-}$ in the melt shows that there is a rather large overpotential for its reduction at the GC surface. This is analogous to the behavior observed in aqueous media. Our laboratory has noted previously that O_2 is capable of oxidizing species with $E^\circ \leq 1.4$ V vs Al/Al(III) in acidic melts, e.g., $Ru(bpy)_3^{2+}$ ($bpy = 2,2'$ -bipyridine).¹⁵ While we have not determined the exact value of E° for the O_2 /products couple in the basic melt, it must be more positive than $+0.267$ V vs Al/Al(III).

Double-potential step chronoamperometry, for steps to potentials negative of the CSV peak of Figure 1 (-1.2 V vs Al/Al(III)) gave linear Cottrell plots ($i(t)$ vs $t^{-1/2}$), for step times between 10 and 250 ms. A typical result is shown in Figure 3. The current axis intercepts for reduction were essentially zero in these cases. No reoxidation current was observed for the reverse potential step (i.e., stepping from -1.2 to 0.0 V) at the pulse times investigated. Potential steps were performed at a potential negative enough that interference from heterogeneous electron-transfer kinetics should be precluded. However, we found that integration of the current-time curve (e.g., to quantify adsorption) gave charge $-t^{1/2}$ plots with significantly negative charge intercepts. This indicates that there may still be some kinetic complication to charge transfer, even at -1.2 V. The diffusion coefficient of O_2 in the melt, D , was determined as $1.5 (\pm 0.2) \times 10^{-4}$ cm²/s (based on a 4 e⁻ transfer, e.g., $O_2 + 4e^- + 4HCl \rightleftharpoons 2H_2O + 4Cl^-$) and $[O_2] = 0.63$ mM). This is an unusually large value for a small, diffusing species in the melt (absolute viscosity of 0.95:1 melt = 20.6 cP). From the Stokes-Einstein relation, using an aqueous diffusion coefficient of 1.0×10^{-5} cm²/s,¹⁴ we have estimated D in the melt as 4.8×10^{-7} cm²/s (25 °C).

The large, apparent value of D suggests that the mechanism of O_2 reduction in the melt probably involves regeneration of O_2 , e.g.¹⁵⁻¹⁷



where O_2 evolved in disproportionation of the perhydroxyl radical can be reduced further at the electrode surface. Such a reaction

- (12) Achord, J. M.; Hussey, C. L. *Anal. Chem.* **1980**, *52*, 601.
 (13) Sahami, S.; Osteryoung, R. A. *Inorg. Chem.* **1984**, *23*, 2511.
 (14) Winlove, C. P.; Parker, K. H.; Oxenham, R. K. C. *J. Electroanal. Chem. Interfacial Electrochem.* **1984**, *170*, 293.
 (15) Morrison, M. M.; Roberts, J. L.; Sawyer, D. T. *Inorg. Chem.* **1979**, *18*, 1971.
 (16) Coffe, P.; Sawyer, D. T. *Anal. Chem.* **1986**, *58*, 1057.
 (17) Chin, D.-H.; Chiericato, G.; Nanni, E. J.; Sawyer, D. T. *J. Am. Chem. Soc.* **1982**, *104*, 1296.

scheme is typical of the chemical step accompanying O_2 reduction in aprotic solvents containing Brønsted acids.

Attempts were made to conduct voltammetric experiments in the absence of protons, in order to stabilize the $1e^-$ reduction product, $O_2^{\cdot -}$.^{18,19} Protons can be removed from basic melts by heating at 75 °C under vacuum.²⁰ Removal of protons was confirmed by the absence of the characteristic voltammetric wave for proton reduction at ca. -0.2 V using a Pt electrode. However, we found that during the course of saturating the melt with O_2 , proton was introduced to the extent of about 1 mM. This was sufficient to preclude stabilization of superoxide. Given the experimental problems encountered with fouling of the electrode (necessitating its removal from the cell for polishing after each voltammetric scan), it is not possible to maintain a rigorously proton-free melt, over the time required to collect data.

Acknowledgment. The work at SUNY was supported in part by SDIO/IST and managed by the Office of Naval Research; the work at the University of Mississippi was supported by the National Science Foundation.

Registry No. ImCl, 65039-09-0; O_2 , 7782-44-7; $AlCl_3$, 7446-70-0; H^+ , 12408-02-5; $AlCl_4^-$, 17611-22-2; Fe, 7439-89-6; carbon, 7440-44-0.

- (18) Maricle, D. L.; Hodgson, W. G. *Anal. Chem.* **1965**, *37*, 1562.
 (19) Peover, M. E.; White, B. S. *Electrochim. Acta* **1966**, *11*, 1061.
 (20) Nöel, M.; Trulove, P. C.; Osteryoung, R. A. The State University of New York at Buffalo, unpublished results.

Contribution from the Department of Analytical and Physical Chemistry, Rhône-Poulenc Rorer Central Research, 800 Business Center Drive-5, Horsham, Pennsylvania 19044, and Department of Chemistry, Drexel University, Philadelphia, Pennsylvania 19104

Heme Rotational Isomerism Is Not Required for the Production of Q-Band Splitting in the Spectra of Iron-Porphyrin Proteins[†]

Thomas J. DiFeo[†] and Anthony W. Addison^{*}

Received June 19, 1990

The phenomenon of heme orientational isomerism is currently a topic of some interest and is often functionally significant in heme proteins.¹⁻¹¹ It has recently been reported¹² that splitting of the α band (the $Q_{0,0}$ band) in the optical absorption spectra of some reconstituted-heme proteins is due to the presence of superimposed spectra arising from rotational isomers of the porphyrin in the protein. These studies were performed exclusively with non-iron porphyrins, and it was concluded that the proximal histidine can adopt "two different coordination modes" depending on the orientation of the porphyrin in the protein, this conclusion being extended to iron heme proteins as well. While the conclusions presented by the authors indeed appear applicable to closed-shell non-iron porphyrins, another interpretation^{13,14} must be considered regarding the observed splitting of the α band in certain native-heme (iron porphyrin) protein derivatives. Figure 1 depicts the spectra of the $Fe^{II}NO$ derivatives of two heme proteins: *Glycera dibranchiata* hemoglobin major component (Hb_c),¹³⁻¹⁵ a monomeric hemoglobin with the distal (E7) substitution His \rightarrow Leu,¹⁶ and equine myoglobin (Mb), which possesses the archetypal histidine distal residue.¹⁷

^{*} To whom correspondence should be addressed at Drexel University.

[†] Rhône-Poulenc Rorer Central Research.

[‡] Abbreviations: $Hb_c^{II}NO$, nitrosyliron(III) form of *Glycera dibranchiata* monomeric hemoglobin major component; $Mb^{II}CO$, carbonyliron(II) form of equine myoglobin.